457

Transverse stress determination of composite plates

S. S. Phoenix[†], M. Sharma[‡] and S. K. Satsangi[‡†]

*Department of Ocean Engineering and Naval Architecture, Indian Institute of Technology,
Kharagpur-721 302, West Bengal, India*

Abstract. Analysis of transverse stresses at layer interfaces in a composite laminate has always been a challenging task. Composite structures possess highly irregular material properties at layer interfaces, which cause high shear stresses. Classical Plate Theory and First Order Shear Deformation Theory (FSDT) use post computing to calculate transverse stresses. This paper presents Reissner Mixed Variational Theorem (RMVT) based finite element model to carry out layer-wise analysis of composite laminates. Selective integration scheme has been used. The formulation has been validated by solving numerical examples and comparing the results with those published in the literature.

Keywords: laminated composites; layer-wise model; transverse stress; mixed formulation; Reissner Mixed Variational Theorem; C_z^0 requirements.

1. Introduction

Over the last two decades composite materials has occupied a very significant position in the field of engineering structures such as aircraft, ship, boat hulls, bridge decks and other industrial applications. The ever increasing use of structural laminates has created considerable interest in their analysis.

Due to the geometry of laminated composite structures, two dimensional approaches have been extensively used to trace their response. Anisotropic multilayered structures often exhibit both higher transverse shear and transverse normal flexibilities with respect to the in-plane deformability than that of single layered traditional isotropic ones. Recently, considerable amount of research has been conducted towards development of computational models which are capable of predicting local effects of laminated and sandwich composites. Exact three dimensional solutions by Pagano (1969, 1970, 1972) have shown that the transverse stresses and displacements are C^0 continuous functions in the thickness direction. Carrera (1996), Carrera and Demasi(2003) and Aitharaju (1999) referred these facts as C_z^0 requirements.

Many equivalent single-layer models have been published in the literature which furnishes interlaminar continuous transverse shear stresses. Some of them are Murakami (1986) and Toledano (1987). Toledano and Murakami (1987) has considered interlaminar continuous transverse normal

---

† Research Student, E-mail: phoenix@naval.iitkgp.ernet.in
‡ Software Engineer, E-mail: muditpisces@gmail.com
‡† Professor, E-mail: subir@naval.iitkgp.ernet.in

stresses also in the proposed mixed model. However, the accuracy of equivalent single-layer models is problem dependent. Partial layer-wise models (zig-zag plate models) have been developed with the purpose of considering the discrete layer effects of the transverse shear stresses. Some of them can be found in the articles by Di Sciuva (1992), Bhaskar and Varadan (1989), Carrera (2004), Demasi (2005), Lee and Lin (1993), Cho and Paramerter (1993), and Averill and Yip (1996). A review of zig-zag theories based on Murakami's zig-zag function can also be found in the article by Demasi (2005). Since the transverse normal stress and strain effects are disregarded in zig-zag plate models, they are not capable of accurately determining the interlaminar stresses near geometric and material discontinuities, at the free edges, and when the layers have rather different mechanical properties. Furthermore, they require integration of local differential equilibrium equations to provide interlaminar stresses, while their finite element counterparts require C^1 interpolation functions. In contrast to equivalent single-layer laminated models, the layer-wise models assume the displacement fields as C^0-continuous through the laminate thickness. Hence, continuity of interlaminar stresses at the layer interfaces is met. The opportunity of refinement offered by stacking sublayers makes layer-wise models able to accurately capture the local stresses directly from constitutive equations (Reddy and Robbins 1994, Setoodeh and Karami 2004). Mixed layer-wise models for predicting local effects of composite structures have been proposed by Carrera (1997, 1998), Carrera and Parisch (1998), Carrera (2005), Carrera and Ciuffreda (2005) and Demasi (2006).

This paper presents an implementation of finite element method presented by Carrera (2000) based on RMVT (Reissner 1984, 1986). The analysis has been done for multilayered plates subjected to different types of loadings under different boundary conditions. The zig-zag effects and inter laminar continuity requirements (C_z^0 requirements) are met. A computer code has been developed in C-language and the numerical results obtained have been compared with those available in the literature.

2. Finite element formulation

2.1 Geometry and notations for multilayered plates

The geometry and co-ordinate system of the laminated plates having number of layers is shown in Fig. 1. $\xi_k = 2\,z_k / h_k$ is the non-dimensional local layer co-ordinate. The compact notations used in
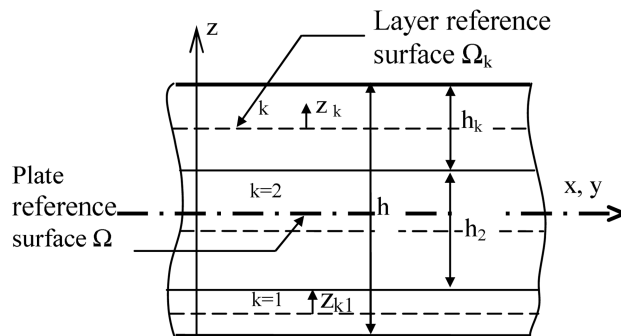

Fig. 1 Geometry and co-ordinate system of laminated plates

this work can be used for the finite element implementation of about 40 theories for the analysis of multilayered composite plates loaded with transverse pressure (Carrera 2005).

2.2 Hooke's law for orthotropic lamina

The material is assumed to be orthotropic. Accordingly $c_{14} = c_{24} = c_{34} = c_{64} = 0$ and $c_{15} = c_{35} = c_{65} = 0$. Thus σ_{13} and σ_{23} depends only on ε_{13} and ε_{23}. In matrix notation, the constitutive equation for a composite lamina may be expressed as

$$
\begin{bmatrix} \sigma_{11} \\ \sigma_{22} \\ \sigma_{12} \\ \sigma_{13} \\ \sigma_{23} \\ \sigma_{33} \end{bmatrix} = \begin{bmatrix} c_{11} & c_{12} & c_{16} & 0 & 0 & c_{13} \\ c_{12} & c_{22} & c_{26} & 0 & 0 & c_{23} \\ c_{16} & c_{26} & c_{66} & 0 & 0 & c_{36} \\ 0 & 0 & 0 & c_{55} & c_{45} & 0 \\ 0 & 0 & 0 & c_{45} & c_{44} & 0 \\ c_{13} & c_{23} & c_{36} & 0 & 0 & c_{33} \end{bmatrix} \begin{bmatrix} \varepsilon_{11} \\ \varepsilon_{22} \\ \varepsilon_{12} \\ \varepsilon_{13} \\ \varepsilon_{23} \\ \varepsilon_{33} \end{bmatrix} ; \quad \text{or} \quad \boldsymbol{\sigma} = \mathbf{C}\boldsymbol{\varepsilon} \tag{1}
$$

For the sake of convenience, Eq. (1) may be partitioned into in-plane and transverse components as

$$
\boldsymbol{\sigma}_p = \begin{bmatrix} \sigma_{11} & \sigma_{22} & \sigma_{12} \end{bmatrix}^T ; \qquad \boldsymbol{\sigma}_n = \begin{bmatrix} \sigma_{13} & \sigma_{23} & \sigma_{33} \end{bmatrix}^T \tag{2}
$$

$$
\boldsymbol{\varepsilon}_p = \begin{bmatrix} \varepsilon_{11} & \varepsilon_{22} & \varepsilon_{12} \end{bmatrix}^T ; \qquad \boldsymbol{\varepsilon}_n = \begin{bmatrix} \varepsilon_{13} & \varepsilon_{23} & \varepsilon_{33} \end{bmatrix}^T \tag{3}
$$

Similarly the $\mathbf{C}$ matrix can be grouped as

$$
\bar{\mathbf{c}}_{pp} = \begin{bmatrix} c_{11} & c_{12} & c_{16} \\ c_{12} & c_{22} & c_{26} \\ c_{16} & c_{26} & c_{66} \end{bmatrix} \qquad \bar{\mathbf{c}}_{nn} = \begin{bmatrix} c_{55} & c_{45} & 0 \\ c_{45} & c_{44} & 0 \\ 0 & 0 & c_{33} \end{bmatrix} \qquad \bar{\mathbf{c}}_{pn} = \begin{bmatrix} 0 & 0 & c_{13} \\ 0 & 0 & c_{23} \\ 0 & 0 & c_{33} \end{bmatrix} = \bar{\mathbf{c}}_{np}^T \tag{4}
$$

With the help of Eqs. (2), (3), and (4), Hooke's law can be rewritten as

$$
\begin{bmatrix} \boldsymbol{\sigma}_p \\ \boldsymbol{\sigma}_n \end{bmatrix} = \begin{bmatrix} \bar{\mathbf{c}}_{pp} & \bar{\mathbf{c}}_{pn} \\ \bar{\mathbf{c}}_{np} & \bar{\mathbf{c}}_{nn} \end{bmatrix} \begin{bmatrix} \boldsymbol{\varepsilon}_p \\ \boldsymbol{\varepsilon}_n \end{bmatrix} ; \quad \boldsymbol{\sigma}_p = \mathbf{c}_{pp}\boldsymbol{\varepsilon}_p + \mathbf{c}_{pn}\boldsymbol{\sigma}_n, \quad \boldsymbol{\varepsilon}_n = \mathbf{c}_{np}\boldsymbol{\varepsilon}_p + \mathbf{c}_{nn}\boldsymbol{\sigma}_n \tag{5}
$$

where

$$
\mathbf{c}_{pp} = \bar{\mathbf{c}}_{pp} - \bar{\mathbf{c}}_{pn}(\bar{\mathbf{c}}_{nn})^{-1}\bar{\mathbf{c}}_{np}; \quad \mathbf{c}_{pn} = \bar{\mathbf{c}}_{pn}(\bar{\mathbf{c}}_{nn})^{-1}; \quad \mathbf{c}_{np} = -(\bar{\mathbf{c}}_{nn})^{-1}\bar{\mathbf{c}}_{np}; \quad \mathbf{c}_{nn} = (\bar{\mathbf{c}}_{nn})^{-1}
$$

Eq. (5) represents the mixed form of Hooke's law.

2.3 Strain-displacement relations

The strain-displacement relationship is

$$
\boldsymbol{\varepsilon}_p = \mathbf{D}_p\mathbf{u}; \quad \boldsymbol{\varepsilon}_n = \mathbf{D}_n\mathbf{u} = (\mathbf{D}_{n\Omega} + \mathbf{D}_{nz})\mathbf{u} \tag{6}
$$

The differential matrices are

$$
\mathbf{D}_p = \begin{bmatrix} \dfrac{\partial}{\partial x} & 0 & 0 \\[2mm] 0 & \dfrac{\partial}{\partial y} & 0 \\[2mm] \dfrac{\partial}{\partial y} & \dfrac{\partial}{\partial x} & 0 \end{bmatrix} \qquad \mathbf{D}_{nz} = \begin{bmatrix} \dfrac{\partial}{\partial z} & 0 & 0 \\[2mm] 0 & \dfrac{\partial}{\partial z} & 0 \\[2mm] 0 & 0 & \dfrac{\partial}{\partial z} \end{bmatrix} \qquad \mathbf{D}_{n\Omega} = \begin{bmatrix} 0 & 0 & \dfrac{\partial}{\partial x} \\[2mm] 0 & 0 & \dfrac{\partial}{\partial y} \\[2mm] 0 & 0 & 0 \end{bmatrix} \tag{7}
$$

2.4 Finite element formulation and shape functions

The field displacements and nodal displacements are connected by

$$
\mathbf{u}_\tau^k = N_i q_{\tau i}^k; \qquad \sigma_{n\tau}^k = N_i g_{\tau i}^k; \qquad (i = 1, 2, \ldots, N_n) \tag{8}
$$

The addition of constraint equation for the transverse stress to the Principle of Virtual Displacement (PVD) leads to RMVT.
RMVT therefore states

$$
\int_v (\delta\boldsymbol{\varepsilon}_{pG}^T \boldsymbol{\sigma}_{pH} + \delta\boldsymbol{\varepsilon}_{nG}^T \boldsymbol{\sigma}_{nM} + \delta\boldsymbol{\sigma}_{nM}^T (\boldsymbol{\varepsilon}_{nG} - \boldsymbol{\varepsilon}_{nH})) \, dV = \delta L_e \tag{9}
$$

The variation of the internal work has been split into in-plane and out-of-plane parts and involves stress from Hooke's law and strain from geometrical relations. δL_e is the virtual variation of the work done by the external force.

2.5 Displacement and transverse stress assumptions for RMVT

The displacement and transverse stress fields along thickness direction are assumed as follows

$$
\mathbf{u}^k = F_t u_t + F_b u_b + F_r u_r = F_\tau u_\tau; \qquad \tau = t, b, r
$$

$$
\sigma_n^k = F_t \sigma_{nt}^k + F_b \sigma_{nb}^k + F_r \sigma_{nr}^k \qquad ; \tag{10}
$$

where

$$
F_b = (P_0 + P_1)/2 = (1 + \zeta_k)/2; \quad F_t = (P_0 - P_1)/2 = (1 - \zeta_k)/2; \quad F_r = (P_r - P_{r-2})/2
$$

It may to be noted that the layer-wise description does not require any zig-zag function for the simulation of zig-zag effects. The continuity of the displacement at each interface can be linked using Eq. (11).

$$
u_t^k = u_b^{(k+1)}, \quad k = 1, N_l - 1 \quad \text{and} \quad \sigma_{nt}^k = \sigma_{nb}^{k+1} \tag{11}
$$

2.6 Finite element matrices for the kth layer

Combining Eqs. (5), (6), (8), and (9), one gets

$$\delta L_e = \delta q^{kT} [\mathbf{K}_{uu}^{k\tau sij} q_s^k + \mathbf{K}_{u\sigma}^{k\tau sij} g^k] + \delta g^{kT} [\mathbf{K}_{\sigma u}^{k\tau sij} q^k + \mathbf{K}_{\sigma\sigma}^{k\tau sij} g^k] \tag{12}$$

where

$$\mathbf{K}_{uu}^{k\tau sij} = \int_\Omega \mathbf{D}_p^T(N_i\mathbf{I})Z_{pp}^{k\tau s}\mathbf{D}_p(N_j\mathbf{I}); \quad \mathbf{K}_{\sigma\sigma}^{k\tau sij} = \int_\Omega -N_i Z_{nn}^{k\tau s} N_j$$

$$\mathbf{K}_{u\sigma}^{k\tau sij} = \int_\Omega (\mathbf{D}_p^T(N_i\mathbf{I})\mathbf{Z}_{pn}^{k\tau s}N_j + \mathbf{D}_{n\Omega}^T(N_i\mathbf{I})E_{\tau s}N_j + E_{\tau_{,z}s}N_i N_j\mathbf{I})$$

$$\mathbf{K}_{\sigma u}^{k\tau sij} = \int_\Omega (N_i E_{\tau s}\mathbf{D}_{n\Omega}(N_i\mathbf{I}) + E_{\tau s_{,z}}N_i N_j\mathbf{I} - N_i Z_{np}^{k\tau s}\mathbf{D}_p(N_j\mathbf{I}))$$

$$(\mathbf{Z}_{pp}^{k\tau s}, \mathbf{Z}_{pn}^{k\tau s}, \mathbf{Z}_{np}^{k\tau s}, \mathbf{Z}_{nn}^{k\tau s}) = (\mathbf{c}_{pp}^k, \mathbf{c}_{pn}^k, \mathbf{c}_{np}^k, \mathbf{c}_{nn}^k)E_{\tau s}$$

$$(E_{\tau s}, E_{\tau s_{,z}}, E_{\tau_{,z}s}, E_{\tau_{,z}s_{,z}}) = \int_{A_k}(F_\tau F_s, F_\tau F_{s_{,z}}, F_{\tau_{,z}}F_s, F_{\tau_{,z}}F_{s_{,z}})dz$$

By imposing the definition of virtual variations, the RMVT leads to the equilibrium and compatibility equations as given in Eqs. (13) and (14).

$$\mathbf{K}_{uu}^{k\tau sij}\mathbf{q}^k + \mathbf{K}_{u\sigma}^{k\tau sij}\mathbf{g}^k = \mathbf{p}^k \tag{13}$$

$$\mathbf{K}_{\sigma u}^{k\tau sij}\mathbf{q}^k + \mathbf{K}_{\sigma\sigma}^{k\tau sij}\mathbf{g}^k = \mathbf{0} \tag{14}$$

The relationship between nodal displacement vector, $\mathbf{q}^k$ and nodal load vector, $\mathbf{p}^k$ may be obtained by eliminating nodal transverse stress vector, $\mathbf{g}^k$ from Eqs. (13) and (14). The resulting equation will be

$$\mathbf{K}_{mixed}\mathbf{q}^k = \mathbf{p}^k \tag{15}$$

where

$$\mathbf{K}_{mixed} = [\mathbf{K}_{uu}^{k\tau sij} - \mathbf{K}_{\sigma u}^{k\tau sij}(\mathbf{K}_{\sigma\sigma}^{k\tau sij})^{-1}\mathbf{K}_{u\sigma}^{k\tau sij}]$$

The elimination of transverse stress unknowns at element level using static condensation technique distorts the continuity of transverse stresses at layer interfaces to a certain extend. This defect can be rectified by solving the full mixed problem without the elimination of transverse stress parameters from the equilibrium and compatibility equations. However, in engineering applications, it was found that the difference between the out-of-plane stresses calculated with and without elimination of transverse stress unknowns at element level is very small. Elimination of transverse stress parameters at element level results significant reduction in CPU time and hence it has to be preferred in the application of RMVT (Demasi 2006). Therefore, in the present work, transverse stress parameters are eliminated at the element level.
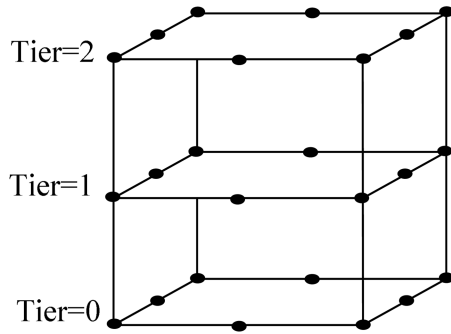
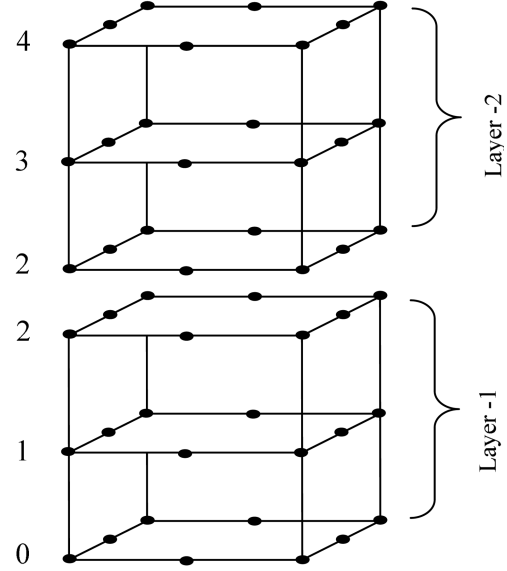Fig. 2 Two dimensional Tiers in an element over one layer

Fig. 3. A laminate element extended over 2 layers

2.7 Assembly of element stiffness matrix from layer to multilayer

For the analysis of composite plates based on RMVT each lamina in a laminate is first divided into n+1 2D-tiers. Tiers are taken as planes parallel to the surface of the lamina. The number of divisions of plate along x-direction and y-direction can vary independently of each other.

Stiffness matrices are calculated separately for each tier combination. Each tier has its own unique value of the stiffness matrices depending upon their interpolation function values along the thickness direction. Fig. 2 shows placing of tiers in an element for one-layer with second order variation of displacements and transverse stresses along thickness. Several such elements are stacked one above the other for getting the element extended over the entire plate thickness. Fig. 3 shows assembling of elements from layer to multi-layer level. After obtaining the stiffness matrix, $\mathbf{K}_{mixed}$ and load vector for an element extended over the full thickness of the plate it has to be assembled along the in-plane direction to form the overall stiffness matrix and load vector of the whole system. Thus the governing equation of the system is obtained which is similar to the Eq. (15). Next the boundary conditions are implemented. Finally, the governing equations are solved to yield the nodal parameters of the whole system.

3. Numerical examples

Analysis has been done for orthotropic multilayered thin, moderately thick, thick and very thick plates under different loadings with simply supported boundary condition. The order of variation of displacement and transverse stress fields along the thickness direction are taken as four, if not specified. Analysis of thin plates with present plate element using full integration scheme reduces
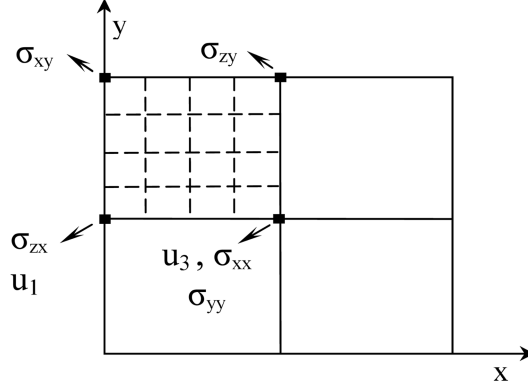
Fig. 4 Finite Element Model of quarter plate

accuracy in results due to shear locking. To avoid shear locking in thin plates, the reduced and selective reduced integration techniques were proposed in (Zienkiewicz *et al.* 1971, Pawsey and Clough 1971, Briassoulis 1989). The reduced integration procedure is the reduction in the order of integration in computing the stiffness matrix of the finite element. Similarly, the selective integration procedure is also a kind of reduced integration rule which is used to evaluate the stiffness matrix associated with the troublesome shear strain energy. Therefore, in order to avoid shear locking in the present analysis reduced integration (2×2) has been done for terms which are related to the transverse shear strain energy as suggested in (Carrera and Demasi 2002). The stresses and displacements are non-dimensionalized according to the following formulas. Finite element model of quarter plate used for the analysis is shown in Fig. 4. It also indicates the locations at which stresses and displacements are calculated.

$$\overline{U}_z = U_z \frac{100 E_2 h^3}{P_z a^4}; \quad (\overline{\sigma}_{zy}, \overline{\sigma}_{zx}) = \frac{(\sigma_{zy}, \sigma_{zx})}{P_z(a/h)}; \quad \overline{\sigma}_{zz} = \frac{\sigma_{zz}}{P_z}; \quad \overline{U}_x = \frac{u_x E_2}{p_z h};$$

$$(\sigma'_{xx}, \sigma'_{yy}, \sigma'_{xy}) = \frac{(\sigma_{xx}, \sigma_{yy}, \sigma_{xy})}{p_z}; \quad (\overline{\sigma}_{xx}, \overline{\sigma}_{yy}, \overline{\sigma}_{xy}) = \frac{(\sigma_{xx}, \sigma_{yy}, \sigma_{xy})}{P_z(a/h)^2}$$

Example-1

The problem of simply supported symmetric and anti-symmetric cross ply laminate is studied for different span to thickness ratios (a/h) of 2 to 100 under bi-sinusoidal loading ($P = P_z \sin(\pi x/a)\sin(\pi y/b)$). Even though the individual layers possess different orientation, they have equal thickness and material properties. ($E_1/E_2 = 25$; $G_{12} = G_{13} = 0.5 * E_2$; $G_{23} = 0.2 * E_2$; $\upsilon_{12} = \upsilon_{23} = 0.25$; $\upsilon_{13} = 0.01$). The results obtained are compared in Tables 1, 2 and in Figs. 5(a)-(c) along with the three dimensional solution presented by Pagano (1969) and those presented by Carrera and Demasi (2002). In-plane stresses calculated with 2nd order and 4th order variation of displacement and transverse stresses along thickness direction are plotted in Fig. 5.

Table 1 Comparison of results for an anti-symmetric laminate (0/90/0/90)

a/h	Method	$\overline{\sigma}_{zx}$ ($z = 0$)	$\overline{\sigma}_{zy}$ ($z = 0$)	$\overline{\sigma}_{zz}$ ($z = 0$)	$\overline{U}_z$ ($z = 0$)
	3D (Pagano1969)	0.1625	0.1947	0.4512	5.2632
2	FEM (LM4)* (Carrera and Demasi 2002)	0.1727	0.2058	0.4512	5.2642
	Present FEM (LM4)	0.1680	0.2014	0.4629	5.2622
	3D (Pagano1969)	0.2713	0.2719	0.4996	0.7623
10	FEM (LM4) (Carrera and Demasi 2002)	0.2638	0.2645	0.5015	0.7629
	Present FEM (LM4)	0.2781	0.2788	0.5121	0.7623
	3D (Pagano1969)	0.2803	0.2803	0.5000	0.5092
100	FEM (LM4) (Carrera and Demasi 2002)	0.3032	0.3033	0.5302	0.5094
	Present FEM (LM4)	0.2871	0.2871	0.5083	0.5091

*Layer-wise model with 4th order variation of displacement and transverse stresses

Table 2 Comparison of results for a symmetric laminate (0/90/90/0)

a/h	Method	$\overline{\sigma}_{zx}$ ($z = 0$)	$\overline{\sigma}_{zy}$ ($z = 0$)	$\overline{\sigma}_{zz}$ ($z = 0$)	$\overline{U}_z$ ($z = 0$)
	3D (Pagano1969)	0.1530	0.2950	-	5.075
2	FEM (LM4)* (Carrera and Demasi 2002)	0.1601	0.3105	0.4576	5.0800
	Present FEM (LM4)	0.1584	0.3024	0.4695	5.0734
	3D (Pagano1969)	0.2190	0.2920	-	1.9370
4	FEM (LM4) (Carrera and Demasi 2002)	0.2294	0.3148	0.4964	1.9374
	Present FEM (LM4)	0.2251	0.2990	0.5083	1.9365
	3D (Pagano1969)	0.3010	0.1960	-	0.7370
10	FEM (LM4) (Carrera and Demasi 2002)	0.3073	0.1607	0.5018	0.7376
	Present FEM (LM4)	0.3090	0.2010	0.5124	0.7370
	3D (Pagano1969)	0.3280	0.1560	-	0.5123
20	FEM (LM4) (Carrera and Demasi 2002)	0.3592	0.1697	0.5342	0.5133
	Present FEM (LM4)	0.3365	0.1560	0.5122	0.5123
	3D (Pagano1969)	0.3370	0.1410	-	0.4460
50	FEM (LM4) (Carrera and Demasi 2002)	0.3665 (8.75%)	0.1533	0.5305	0.4449
	Present FEM (LM4)	0.3450	0.1440	0.5100	0.4445
	3D (Pagano1969)	0.3390	0.1390	-	0.4350
100	FEM (LM4) (Carrera and Demasi 2002)	0.3665	0.1505 (8.27%)	0.5302	0.4348
	Present FEM (LM4)	0.3470	0.1426	0.5083	0.4343
	3D (Pagano1969)	-	-	-	-
1000	FEM (LM4) (Carrera and Demasi 2002)	0.3663	0.1496	0.5301	0.4315
	Present FEM (LM4)	0.3639	0.1871	0.5076	0.4154

*Layer-wise model with 4th order variation of displacement and transverse stresses
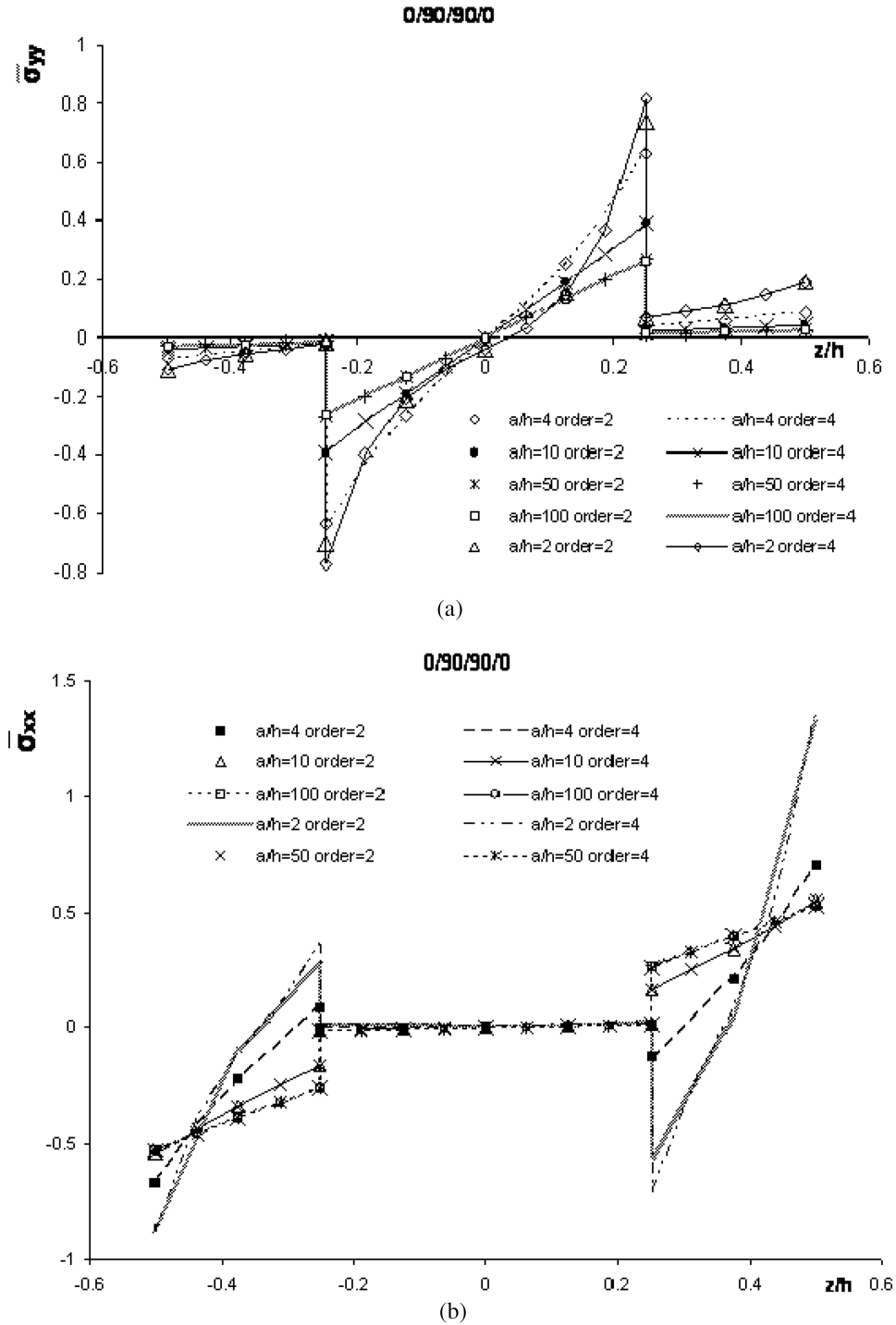
(a)

(b)

Fig. 5 Variation of in-plane stress along the thickness direction for a symmetric plate under bi-sinusoidal loading
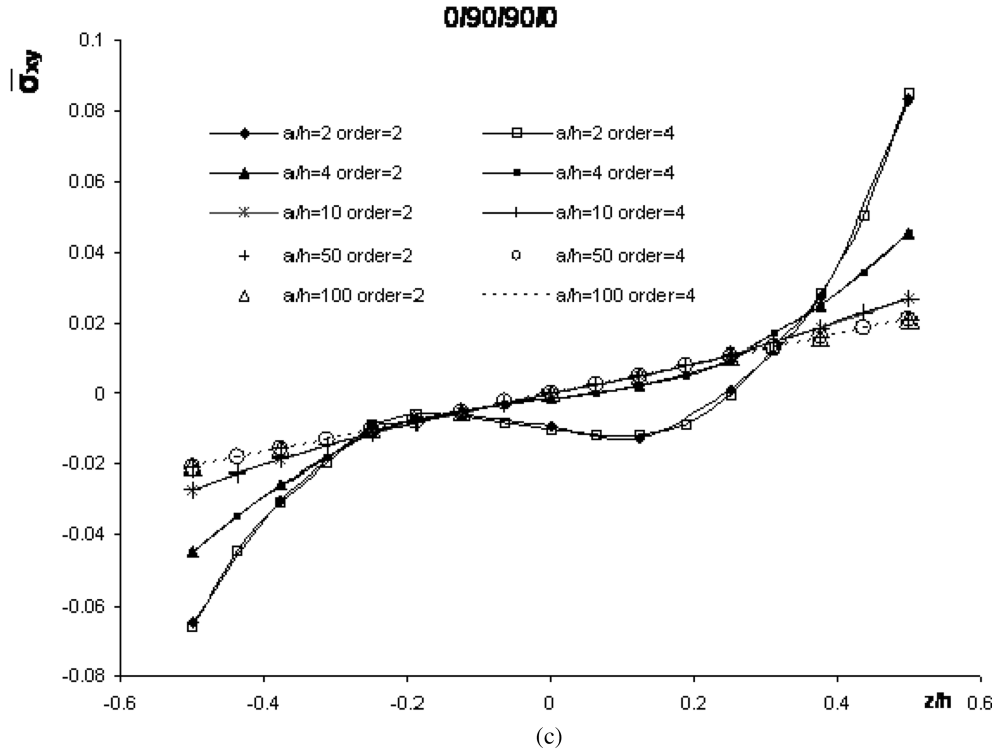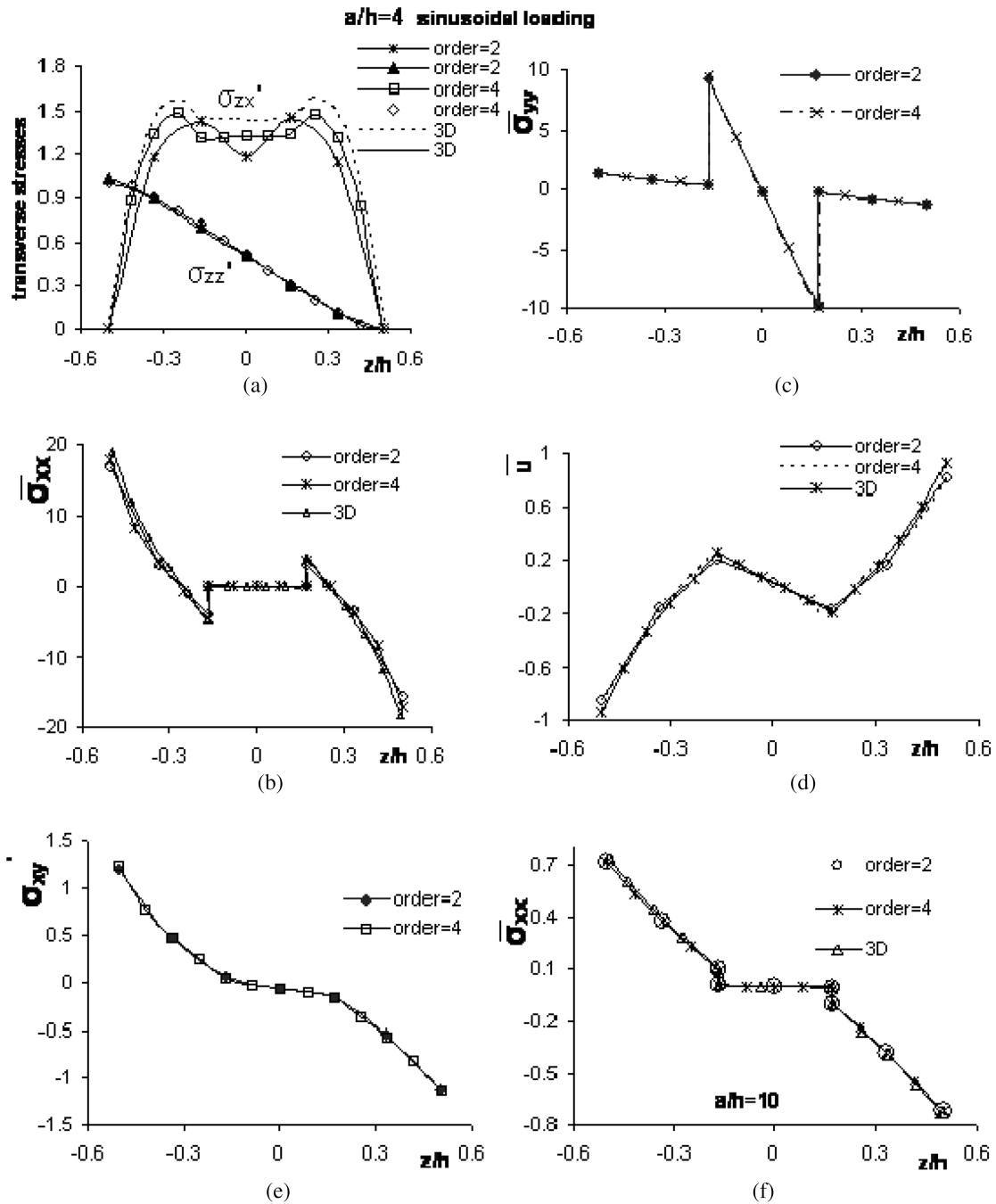
Fig. 5 Continued

Example-2

A three ply simply supported laminate (0/90/0) with span to thickness ratios (a/h) of 4 and 100 under sinusoidal loading ($P = P_z \sin(\pi x/a)$) and under bi-sinusoidal loading ($P = P_z \sin(\pi x/a)$ $\sin(\pi y/b)$) has been analyzed. Due to geometric, material and loading symmetry, only one quarter of the plate was considered. The analysis has been done with an eight-noded isoparametric element with 2nd order and 4th order variation of displacement and transverse stress fields along thickness direction. The results are compared in Figs. 6(a)-(n) with the exact solution of Pagano (1969) and with the solution obtained from Carrera (2002). The material properties are: $E_1/E_2 = 25$; $G_{12} = G_{13} = 0.5 * E_2$; $G_{23} = 0.2 * E_2$; $\upsilon_{12} = \upsilon_{23} = 0.25$; $\upsilon_{13} = 0.01$ and $h_1 = h_3 = h_2 = h/3$.

Example-3

Analysis for symmetric and anti-symmetric cross ply laminate is studied for different span to thickness ratios (a/h) of 2 to 100 under uniformly distributed load as well as sinusoidal loading ($P = P_z \sin(\pi x/a)$) has been done and the results are tabulated in Table 3 and Table 4. The material properties are: $E_1/E_2 = 25$; $G_{12} = G_{13} = 0.5 * E_2$; $G_{23} = 0.2 * E_2$; $\upsilon_{12} = \upsilon_{23} = 0.25$; $\upsilon_{13} = 0.01$ and $h_1 = h_2 = h_3 = h_4 = h/4$.

Fig. 6 Variation of stresses and displacement along the thickness direction for a laminated plate (0/90/0) under simply supported boundary conditions
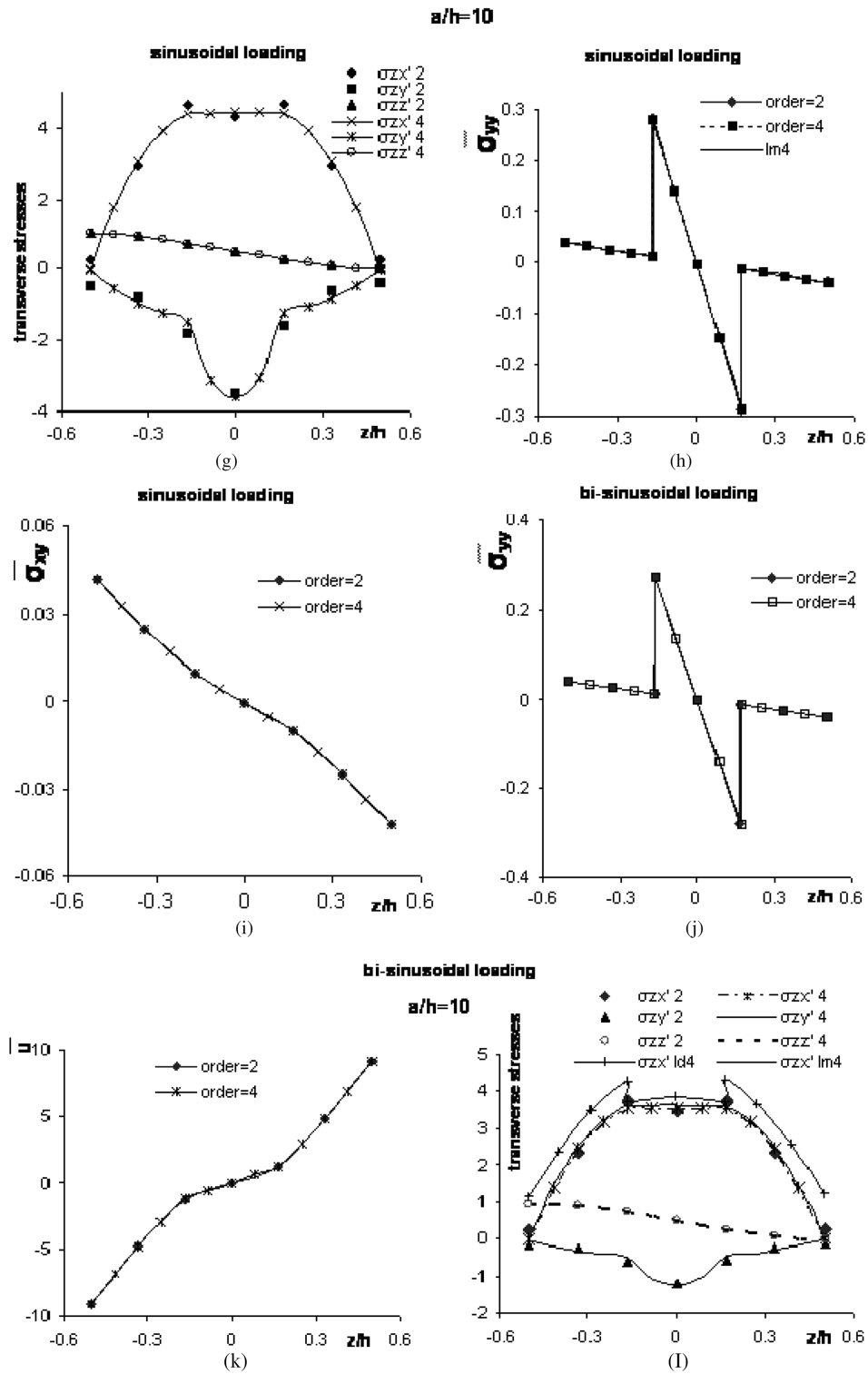
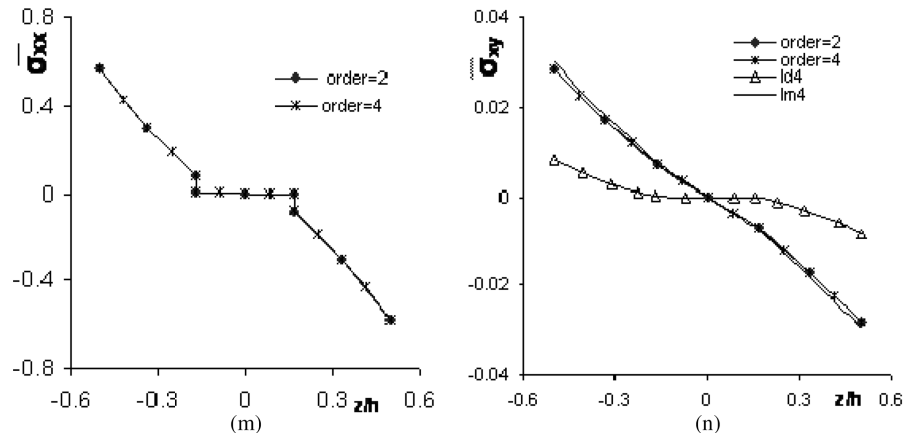*Equivalent single layer model with 4th order variation of displacement field.
**Layer-wise model with 4th order variation of displacement and transverse stress fields.

a/h=10

(g)

(h)

(i)

(j)

(k)

(I)

Fig. 6 Continued

Fig. 6 Continued

Table 3 Non-dimensional stresses and deflection values for symmetric laminate calculated using LM4

Model	Loading	a/h	$\overline{\sigma}_{xx}$ $(\pm h/2)$	$\overline{\sigma}_{yy}$ $(\pm h/4)$	$\overline{\sigma}_{xy}$ $(\pm h/2)$	$\overline{\sigma}_{zx}$ $(z = 0)$	$\overline{\sigma}_{zy}$ $(z = 0)$	$\overline{\sigma}_{zz}$ $(z = 0)$	$\overline{U}_z$ $(z = 0)$
0/90/90/0	Sinusoidal loading	2	1.1375 −1.6327	0.9772 −0.9502	−0.0899 0.1477	0.1927	−0.4593	0.4962	6.2200
		10	0.6947 −0.6957	0.4422 −0.4442	−0.0387 0.0388	0.3789	−0.4374	0.5056	0.9126
		20	0.6758 −0.6762	0.3265 −0.3270	−0.0322 0.0321	0.4128	−0.4089	0.5115	0.6365
		50	0.6715 −0.6716	0.2858 −0.2859	−0.0301 0.0301	0.4244	−0.4029	0.5104	0.5524
		100	0.6709 −0.8709	0.2796 −0.2796	−0.0298 0.0298	0.4257	−0.4032	0.5058	0.5400
0/90/90/0	Uniformly distributed load	2	1.6327 −1.1375	0.9771 −0.9502	−0.0899 0.1478	0.1927	−0.4593	0.4065	6.2210
		10	0.8306 −0.8287	0.5596 −0.5618	−0.0549 0.0561	0.5721	−0.5109	0.4979	1.1410
		20	0.8248 −0.8244	0.4160 −0.4160	−0.0442 0.0441	0.6294	−0.4788	0.5083	0.8029
		50	0.8258 −0.8257	0.3643 −0.3644	−0.0401 0.0401	0.6530	−0.4742	0.5121	0.6998
		100	0.8260 −0.8260	0.3563 −0.3563	−0.0395 0.0395	0.6569	−0.4742	0.5038	0.6847

Example-4

A sandwich plate (f/c/f) subjected to localized uniformly distributed load of 1.0 MPa at the centre as shown in Fig. 7 is considered in this example. Analysis has been done with simply supported and clamped boundary conditions. The material properties for the face and core are $E_1 = 70000$ MPa; $E_2 = 71000$ MPa; $E_3 = 69000$ MPa; $E_{12} = E_{13} = E_{23} = 26000$ MPa; $\upsilon_{12} = \upsilon_{23} = 0.3$ and $E_1 = E_2 = $

Table 4 Non-dimensional stresses and deflection values for anti-symmetric laminate calculated using LM4

Model	Loading	a/h	$\overline{\sigma}_{xx}$ $(\pm h/2)$	$\overline{\sigma}_{yy}$ $(\pm h/4)$	$\overline{\sigma}_{xy}$ $(\pm h/2)$	$\overline{\sigma}_{zx}$ $(z = 0)$	$\overline{\sigma}_{zy}$ $(z = 0)$	$\overline{\sigma}_{zz}$ $(z = 0)$	$\overline{U}_z$ $(z = 0)$
0/90/0/90	Sinusoidal loading	2	0.2306 −1.1902	0.0320 −0.9437	−0.0923 0.1288	0.2079	−0.3476	0.3365	6.4839
		4	0.1050 −0.8727	0.0177 −0.7269	−0.0631 0.0672	0.2919	−0.3943	0.5207	2.4131
		10	0.0556 −0.6628	0.0145 −0.5798	−0.4030 0.4030	0.3431	−0.4676	0.5453	0.9486
		20	0.0476 −0.6274	0.0139 −0.5578	−0.0351 0.0350	0.3554	−0.4995	0.5616	0.7175
		50	0.0453 −0.6181	0.0138 −0.5521	−0.0333 0.0333	0.3597	−0.5185	0.5659	0.6521
		100	0.0450 −0.6168	0.0138 −0.5512	−0.0329 0.0330	0.3617	−0.5230	0.5600	0.6427
0/90/0/90	Uniformly distributed load	2	0.2364 −1.4182	0.0283 −1.1786	−0.1233 0.2518	0.3009	−0.3685	0.5300	7.9506
		4	0.1135 −1.0044	0.0177 −0.9084	−0.0891 0.1112	0.4362	−0.4663	0.5071	2.9732
		10	0.0635 −0.7761	0.0170 −0.7295	−0.0575 0.0587	0.5474	−0.5566	0.4981	1.1825
		20	0.0563 −0.7460	0.0170 −0.7066	−0.0485 0.0484	0.5929	−0.5961	0.5082	0.9024
		50	0.0545 −0.7395	0.0170 −0.7020	−0.045 0.045	0.6166	−0.6174	0.5121	0.8235
		100	0.0543 −0.7386	0.0170 −0.7014	−0.0442 0.0442	0.6209	−0.6211	0.5039	0.8123
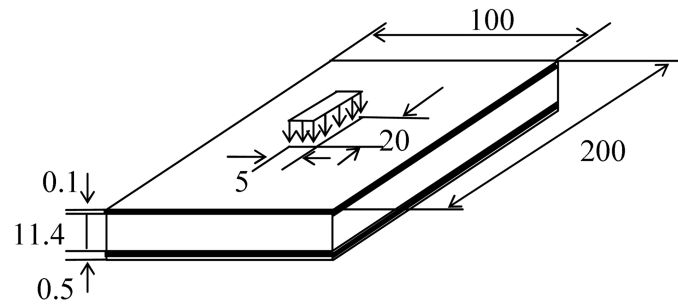
Fig. 7 Sandwich plate subjected to uniformly distributed load at the centre

3 MPa; $E_3 = 2.8$ MPa; $E_{12} = E_{13} = E_{23} = 1$ MPa; $\upsilon_{12} = \upsilon_{23} = 0.25$ respectively. The values of central deflection and in-plane stresses obtained in the present analysis along with the solutions presented by Carrera and Demasi (2003) are tabulated in Table 5. The absolute values of error presented in Table 5 are calculated with respect to the three-Dimensional solutions.

Table 5 Stresses and deflection values for sandwich plate

Analysis			All edges simply supported				All edges clamped	
			Top face	Error (%)	Bottom face	Error (%)	Top face	Bottom face
U_z	3D analytical (Carrera and Demasi 2003)		−3.7800	-	−2.1400	-	-	-
	FEM (LM2*) (Carrera and Demasi 2003)		−3.7628	0.46	−2.1900	2.34	-	-
	FEM (ED1†) (Carrera and Demasi 2003)		−0.0187	99.51	−0.0181	99.15	-	-
	Present FEM (LM2)		−3.7629	0.45	−2.1400	0.00	−3.5450	−1.9220
σ_{xx}	3D analytical (Carrera and Demasi 2003)	Top	−624.00	-	−241.00	-	-	-
		Bottom	580.00	-	211.00	-	-	-
	FEM (LM2) (Carrera and Demasi 2003)	Top	−595.56	4.56	−223.93	7.08	-	-
		Bottom	556.00	4.14	196.37	6.93	-	-
	FEM (ED1) (Carrera and Demasi 2003)	Top	−29.460	95.28	−23.990	90.05	-	-
		Bottom	−29.170	105.03	−23.750	111.26	-	-
	Present FEM (LM2)	Top	−632.223	1.32	−225.25	6.54	−519.480	−144.070
		Bottom	590.375	1.79	195.775	7.22	483.541	139.004
σ_{yy}	3D analytical (Carrera and Demasi 2003)	Top	−138.00	-	−121.00	-	-	-
		Bottom	146.00	-	127.00	-	-	-
	FEM (LM2) (Carrera and Demasi 2003)	Top	−136.20	1.30	−118.99	1.66	-	-
		Bottom	144.03	1.35	125.00	1.57	-	-
	FEM (ED1) (Carrera and Demasi 2003)	Top	4.8700	103.53	3.3200	102.74	-	-
		Bottom	6.3600	95.64	4.5000	96.46	-	-
	Present FEM (LM2)	Top	−138.515	0.37	−121.038	0.03	−209.392	124.096
		Bottom	146.304	0.21	127.149	0.12	177.431	118.693

*Layer-wise model based on RMVT with 2nd order expansion for displacement and transverse stress.
†Equivalent single layer model based on Principle of virtual displacement theory
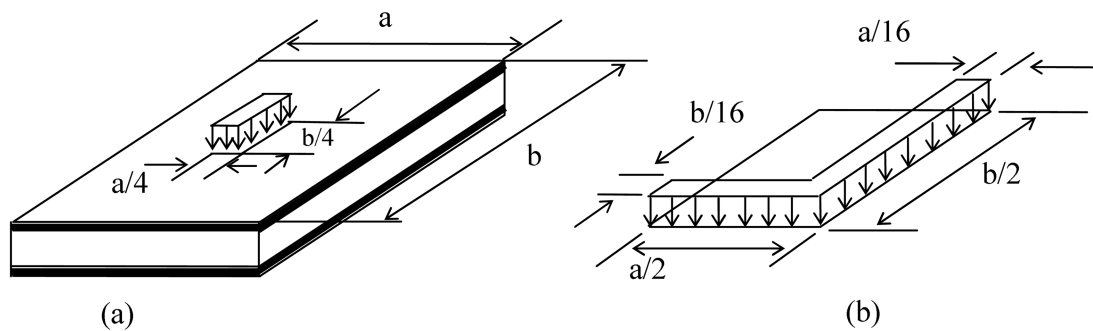

Fig. 8 Sandwich plate subjected to localized loads at the top surface

Example-5

In this example a simply supported square sandwich plate having geometry and material properties same as that of Pagano (1970) is studied with different span to depth ratios under of

Table 6 Stresses and deflection values of sandwich plate for different span to depth ratios calculated using LM2

Type of loading		$a/h = 4$				$a/h = 10$				$a/h = 50$				a/h = 100			
		L1	L2	L3	L4	L1	L2	L3	L4	L1	L2	L3	L4	L1	L2	L3	L4
$\overline{U}_z$	$h/2$	4.430	9.217	8.007	6.652	0.747	2.004	1.692	1.403	0.274	0.814	0.681	0.571	0.259	0.775	0.648	0.545
	$-h/2$	1.398	5.301	4.339	3.545	0.652	1.919	1.606	1.310	0.274	0.814	0.681	0.571	0.259	0.775	0.648	0.545
$\overline{\sigma}_{xx}$	$h/2$	1.511	1.735	1.636	1.122	0.461	1.023	0.881	0.693	0.382	0.985	0.834	0.662	0.381	0.983	0.832	0.659
	$0.4h$	−1.065	−0.530	−0.619	−0.326	0.111	0.564	0.455	0.380	0.295	0.776	0.656	0.523	0.302	0.783	0.663	0.526
		0.017	0.020	0.019	0.018	0.004	0.005	0.005	0.0043	0.0009	0.0019	0.0016	0.0014	0.0008	0.0018	0.0015	0.0013
	$-0.4h$	−0.001	−0.0006	−0.0006	−0.0008	−0.0005	−0.002	−0.0014	−0.0011	−0.0008	−0.0018	−0.0015	−0.0013	−0.0008	−0.0018	−0.0015	−0.0013
		−0.191	−0.176	−0.177	−0.090	−0.173	−0.569	−0.472	−0.385	−0.296	−0.777	−0.657	−0.523	−0.302	−0.783	−0.663	−0.526
	$-h/2$	−0.249	−1.137	−0.923	−0.738	−0.415	−1.036	−0.881	−0.706	−0.382	−0.985	−0.834	−0.662	−0.381	−0.983	−0.832	−0.659
$\overline{\sigma}_{yy}$	$h/2$	0.189	0.037	0.223	0.235	0.061	0.110	0.0980	0.0833	0.0382	0.0623	0.0566	0.0566	0.037	0.060	0.055	0.0565
	$0.4h$	0.0038	0.136	0.103	0.044	0.041	0.082	0.0719	0.0574	0.0304	0.0497	0.0451	0.0448	0.0294	0.0483	0.044	0.0451
		0.018	0.025	0.023	0.0198	0.005	0.007	0.0061	0.0055	0.0014	0.0022	0.002	0.002	0.0013	0.0021	0.0019	0.0019
	$-0.4h$	−0.004	−0.006	−0.006	−0.005	−0.0017	−0.004	−0.0032	−0.0025	−0.0013	−0.0021	−0.0019	−0.0019	−0.0013	−0.0021	−0.0019	−0.0019
		−0.082	−0.184	−0.158	−0.124	−0.047	−0.090	−0.079	−0.0645	−0.031	−0.050	−0.045	−0.045	−0.0295	−0.0483	−0.044	−0.045
	$-h/2$	−0.700	−0.258	−0.214	−0.153	−0.0685	−0.117	−0.104	−0.0859	−0.0385	−0.0626	−0.0569	−0.0567	−0.0369	−0.061	−0.055	−0.0565
$\overline{\sigma}_{zx}$	$h/2$	0.014	0.026	0.0234	−0.014	−0.0013	−0.005	−0.0037	−0.056	−0.0013	−0.0038	−0.0032	−0.008	−0.0009	−0.0027	−0.0023	−0.001
	$0.4h$	0.046	0.165	0.136	0.239	0.063	0.229	0.1875	0.244	0.0692	0.249	0.205	0.289	0.0679	0.247	0.204	0.297
	$-0.4h$	0.049	0.186	0.152	0.119	0.063	0.227	0.1866	0.215	0.0691	0.249	0.205	0.291	0.0679	0.047	0.204	0.298
	$-h/2$	−0.008	0.025	−0.021	0.002	−0.001	−0.004	−0.003	0.0006	−0.0013	−0.0036	−0.003	−0.004	−0.0009	−0.003	−0.003	−0.0005
$\overline{\sigma}_{zy}$	$h/2$	0.006	0.005	0.006	0.190	0.0014	0.003	0.0024	0.0601	0.0004	0.0016	0.0013	−0.002	0.0004	0.0012	0.001	−0.0046
	$0.4h$	−0.008	−0.029	−0.023	−0.197	0.0032	−0.002	−0.0005	−0.103	0.0032	0.0022	0.0027	−0.0474	0.003	0.0011	0.0019	−0.043
	$-0.4h$	−0.007	−0.052	−0.041	−0.045	0.0034	−0.002	0.00003	−0.0499	0.0032	0.002	0.0024	−0.0482	0.003	0.0012	0.0018	−0.044
	$-h/2$	−0.0003	0.0036	0.003	−0.009	0.001	0.003	0.0023	−0.0034	0.0005	0.0018	0.0015	−0.0009	0.0004	0.0013	0.0011	−0.004
$\overline{\sigma}_{zz}$	$h/2$	0.909	0.997	0.958	1.146	1.000	0.996	0.980	1.069	0.994	0.996	0.980	1.048	0.993	0.997	0.982	1.021
	$0.4h$	0.884	0.962	0.926	0.897	0.981	0.944	0.943	0.933	0.983	0.952	0.944	0.979	0.960	0.951	0.938	0.988
	$-0.4h$	−0.001	0.078	0.064	0.031	0.0997	0.055	0.0576	0.0738	0.0599	0.0547	0.055	0.065	0.056	0.060	0.0589	0.0786
	$-h/2$	0.004	0.007	0.006	0.003	0.006	0.004	0.004	0.006	0.003	0.0015	0.0022	0.021	0.002	0.003	0.0028	0.051

localised loadings. Four different types of loads are considered and they are Uniformly Distributed Load (UDL) at the centre of the plate as in Fig. 8(a) (L1), UDL same as L1 distributed over an area of $a/2 * b/2$ at the centre (L2), Bi-sinusoidal load ($P = P_z \sin(\pi x/a) \sin(\pi y/b)$) distributed over an area of $a/2 * b/2$ at the centre (L3), and a line loading at the center of the plate (L4). A quarter of the plate with line loading considered (L4) is shown in Fig. 8(b). The maximum values of non-dimensionalised displacement and stress fields are tabulated in Table 6.

4. Conclusions

From the present work, it is observed that RMVT is an effective tool to analyze multilayered structures. RMVT leads to a quasi-three-dimensional description of the stress fields of layered plates. In the present formulation, the C_z^0 requirements are satisfied *a priori* and no post processing operations are required to calculate transverse stresses. A computer code has been developed in C programming language to analyze different numerical examples. The results obtained are compared with the existing results and are found to be in good agreement. It is also concluded that use of serendipity elements and selective integration scheme is more effective than that of quadratic element with different integration schemes.

References

Aitharaju, V.R. (1999), "C_z^0 zig-zag finite element for analysis of laminated composite beams", *J. Eng. Mech.*, **125**, 323-330.

Averill, R.C. and Yip, Y.C. (1996), "Development of simple, robust finite elements based on refined theories for thick laminated beams", *Comput. Struct*, **59**, 529-546.

Bhaskar, K. and Varadan, T.K. (1989), "Refinement of higher-order laminated plate theories", *AIAA J.*, **27**, 1830-1831.

Briassoulis, D. (1989), "On the basics of the shear locking problem of C^0 isoparametric plate elements", *Comput. Struct.*, **33**, 169-185.

Carrera, E. (1996), "C^0 Reissner - Mindlin multilayered plate elements including zig-zag and inter laminar stress continuity", *Int. J. Numer. Meth. Eng.*, **39**, 1797-1820.

Carrera, E. (1997), "C_z^0 Requirements - Models for the two dimensional analysis of multilayered structures", *Comput. Struct.*, **37**, 373-383.

Carrera, E. (1998), "Evaluation of layer-wise mixed theories for laminated plates analysis", *AIAA J.*, **36**, 830-839.

Carrera, E. (2000), "A priori vs. a posteriori evaluation of transverse stresses in multilayered orthotropic plates", *Compos. Struct.*, **48**, 245-260.

Carrera, E. (2003), "Historical review of zig-zag theories for multilayered plates and shells", *Appl. Mech. Rev*, **56**, 287-308.

Carrera, E. (2004), "On the use of Murukami's zig-zag function in the modeling of layered plates and shells", *Comput. Struct.*, **82**, 541-554.

Carrera, E. (2005), "A unified formulation to assess theories of multilayered plates for various bending problems", *Compos. Struct.*, **69**, 271-293.

Carrera, E. and Ciuffreda, A. (2005), "Bending of composites and sandwich plates subjected to localized lateral loadings: A comparison of various theories", *Compos. Struct.*, **68**, 185-202.

Carrera, E. and Demasi, L. (2002), "Classical and advanced multilayered plate elements based upon PVD and RMVT. Part 2: Numerical implementations", *Int. J. Numer. Meth. Eng.*, **55**, 253-291.

Carrera, E. and Demasi, L. (2003), "Two benchmarks to assess two-dimensional theories of sandwich, composite

plates", *AIAA*, **41**(7), 1356-1362.

Carrera, E. and Parisch, H. (1998), "An evaluation of geometrical nonlinear effects of thin and moderately thick multilayered composite shells", *Comput. Struct.*, **40**, 11-24.

Cho, M. and Parmerter, R. (1993), "Efficient Higher order composite plate theory for general lamination configurations", *AIAA J.*, **31**, 1299-1306.

Demasi, L. (2005), "Refined multilayered plate elements based on Murakami zig-zag functions", *Compos. Struct.*, **70**, 308-316.

Demasi, L. (2006) "Treatment of stress variables in advanced multilayered plate elements based upon Reissner's mixed variational theorem", *Comput. Struct.*, **84**, 1215-1221.

Demasi, L. (2006), "Quassi-3D analysis of free vibration of anisotropic plates", *Compos. Struct.*, **74**, 449-457.

Di Sciuva, M. (1992), "Multilayered anisotropic plate models with continuous interlaminar stresses", *Compos. Struct.*, **22**, 149-168.

Lee, C.Y. and Liu, D. (1993), "Nonlinear analysis of composite plates using interlaminar shear stress continuity theory", *Compos. Eng.*, **3**, 151-168.

Murakami, H. (1986), "Laminated composite plate theory with improved in-plane response", *J. Appl. Mech.*, **53**, 661-666.

Pagano, N.J. (1969), "Exact solutions for composite laminates in cylindrical bending", *J. Compos. Mater.*, **3**, 398-411.

Pagano, N.J. (1970), "Exact solutions for rectangular bidirectional composites and sandwich plates", *J. Compos. Mater.*, **4**, 20-34.

Pagano, N.J. and Hatfield, S.J. (1972), "Elastic behavior of multilayered bidirectional composites", *AIAA J.*, **10**, 931-933.

Pawsey, S.F. and Clough, R.W. (1971), "Improved numerical integration ofthick shell finite elements", *Int. J. Numer Meth. Eng.*, **3**, 575-586.

Reddy, J.N. and. Robbins Jr. D.H. (1994), "Theories and computational models for composite laminates", *Appl. Mech. Rev.*, **47**, 147-169.

Reissner, E. (1984), "On a certain mixed variational theory and a proposed applications", *Int. J. Numer. Meth. Eng.*, **20**, 1366-1368.

Reissner, E. (1986), "On a mixed variational theorem and on a shear deformable plate theory", *Int. J. Numer. Meth. Eng.*, **23**, 193-198.

Setoodeh, A.R. and Karami, G. (2004), "Static, free vibration and buckling analysis of anisotropic thick laminated composite plates on distributed and point elastic support using a 3D Layerwise FEM", *Eng. Struct.*, **26**, 211-220.

Toledano, A. and Murakami, H. (1987), "A higher-order laminated plate theory with improved in-plane responses", *Int. J. Solids Struct.*, **23**, 111-131.

Zienkiewicz, O.C., Taylor, R.L. and Too, J.M. (1971), "Reduced integration technique in general analysis of plates and shells", *Int. J. Numer Meth. Eng.*, **3**, 275-290.

Notation

a	: shorter length of the plate
A_k	: area of kth layer
b (subscript)	: parameters related to layer bottom
C	: elastic constant matrix
D	: differential operator matrix
E	: Young's modulus
F_τ	: functions of coefficients of Legendre polynomial
g	: transverse stress vector at nodes
G (subscript)	: values calculated from geometrical relations
h	: thickness of the plate
H (subscript)	: values calculated from Hooke's Law

h_k	: thickness of kth layer
I	: unit matrix
i, j (sub/superscript)	: number of node's expansions
k (sub/superscript)	: parameters related to k^{th} layer
L_e	: work done due to external loads
M (subscript)	: values calculated from assumed model
n (subscript)	: out-of-plane values
N_i	: interpolation function corresponding to i^{th} node of plate element
N_l	: number of layers of the plate
N_n	: number of nodes
p	: load vector
P_z	: amplitude of transverse applied pressure
p (subscript)	: in-plane values
P_r	: coefficients of Legendre polynomial
q	: nodal displacement vector
t (subscript)	: parameters related to layer top
u	: displacement vector
V	: plate volume
x, y, z	: cartesian co-ordinates reference systems used for plates
z_k	: thickness co-ordinate for k^{th} layer
ξ_k	: non-dimensional local layer co-ordinate
$\boldsymbol{\sigma}$	: stress vector
τ, s (sub/superscript)	: expansion of parameters along thickness direction
υ	: Poisson's ratio
Ω	: plate reference surface
Ω_k	: layer reference surface
$\boldsymbol{\varepsilon}$	: strain vector